

Original Research

# The Application of Three-dimensional Shear Wave Elastography in the Detection of Inguinal Lymph Node Metastasis in Gynecological Malignancies

Yuping Shen<sup>1</sup>, Jiulong Dai<sup>1</sup>, Jiami Li<sup>2</sup>, Man Lu<sup>1,\*</sup>

Academic Editor: Samir A. Farghaly

Submitted: 26 October 2024 Revised: 13 December 2024 Accepted: 19 December 2024 Published: 17 January 2025

#### Abstract

Background: Accurate assessment of lymph node involvement is essential for prognosis and guiding treatment decisions in gynecological cancers, as it directly influences therapeutic strategies and patient outcomes. However, conventional imaging techniques, such as ultrasound and computed tomography (CT), demonstrate limited accuracy in determining the nature of lymph nodes. This study implements three-dimensional shear wave elastography (3D-SWE), an innovative technique that quantifies the stiffness of inguinal lymph nodes (ILN) in patients with gynecological cancers. This approach offers a more comprehensive assessment of ultrasound elastography compared to traditional methods. Methods: This retrospective study evaluated 120 ILNs from patients with gynecological cancers who underwent conventional ultrasound (US), two-dimensional shear wave elastography (2D-SWE), and multiplanar 3D-SWE. The diagnostic performance was analyzed using receiver operating characteristic (ROC) methodology, enabling a comprehensive comparison of the sensitivity and specificity of 3D-SWE relative to conventional ultrasound and 2D-SWE. Pathology results from lymph node resections or biopsies served as the reference standard. Results: Final pathology confirmed 65 metastatic and 55 benign lymph nodes. The maximum (Emax) and average (Emean) elasticity values from 2D-SWE and 3D-SWE for malignant lymph nodes were significantly higher than those for benign lymph nodes (p < 0.0001). ROC analysis indicated that for identifying metastatic lymph nodes, the area under the curve (AUC) values were 0.798 for 2D-SWE Emax, and 0.828, 0.839, and 0.816 for the transverse, sagittal, and coronal planes of 3D-SWE Emax, respectively. The differences between these AUC values were not statistically significant (p > 0.05). Furthermore, Emax values consistently surpassed Emean values in terms of characterization accuracy across modalities. Although no significant differences were observed between 2D-SWE and 3D-SWE, the sagittal view Emax yielded the best AUC, indicating optimal diagnostic precision overall. Conclusions: 3D-SWE, particularly using the sagittal Emax parameter, effectively distinguishes benign lymph nodes from metastatic ones by quantitatively evaluating the stiffness of ILNs in relation to gynecological tumors. Serving as a dependable diagnostic method for lymph nodes, 3D-SWE may help reduce the necessity for invasive biopsy procedures in some cases.

**Keywords:** two-dimensional shear wave elastography; three-dimensional shear wave elastography; ultrasonography; shear wave elastography; elasticity imaging techniques; gynecologic neoplasms; lymphatic metastasis

#### 1. Introduction

Gynecological cancers pose a significant threat to women's health globally [1]. Cervical cancer ranks as the fourth most prevalent cancer among women [2,3]. Furthermore, the age-standardized incidence and mortality rates of endometrial cancer continue to rise [4–6]. Ovarian cancer remains a leading cause of gynecological cancer-related mortality, frequently diagnosed at an advanced stage [7,8]. Additionally, there has been a consistent increase in the incidence of vulvar intraepithelial neoplasia and vulvar cancer among older women [9,10]. The inguinal lymph nodes (ILN) serve as critical sites for metastasis in vulvar and ovarian cancers, and they may also be involved in the rare metastatic spread of endometrial cancer via the round ligament [11]. For these gynecological malignancies, precise evaluation of ILN status is essential for accurate stag-

ing, prognostication, and for guiding optimal treatment strategies, including lymphadenectomy and adjuvant therapy [10–12]. Consequently, there is an urgent need for accurate, non-invasive imaging diagnostic tools to assess ILN metastasis.

Conventional imaging techniques such as ultrasonography, computed tomography (CT), and positron emission tomography-CT have been extensively employed to evaluate lymph nodes [13–15]. However, the reliance of these modalities on morphological characteristics, alone may restrict diagnostic accuracy and overlook critical mechanical properties, such as stiffness and deformability, which are crucial for distinguishing malignancy. Elastography, as an advanced ultrasound technique, has been effectively utilized to characterize the elastic properties of organs and tissues across various disease states, including cancer [16–

<sup>&</sup>lt;sup>1</sup>Department of Ultrasound Medical Center, Sichuan Clinical Research Center for Cancer, Sichuan Cancer Hospital & Institute, Sichuan Cancer Center, Affiliated Cancer Hospital of University of Electronic Science and Technology of China, 610000 Chengdu, Sichuan, China

<sup>&</sup>lt;sup>2</sup>School of Medical Imaging, North Sichuan Medical College, 637000 Nanchong, Sichuan, China

<sup>\*</sup>Correspondence: graceof@163.com (Man Lu)

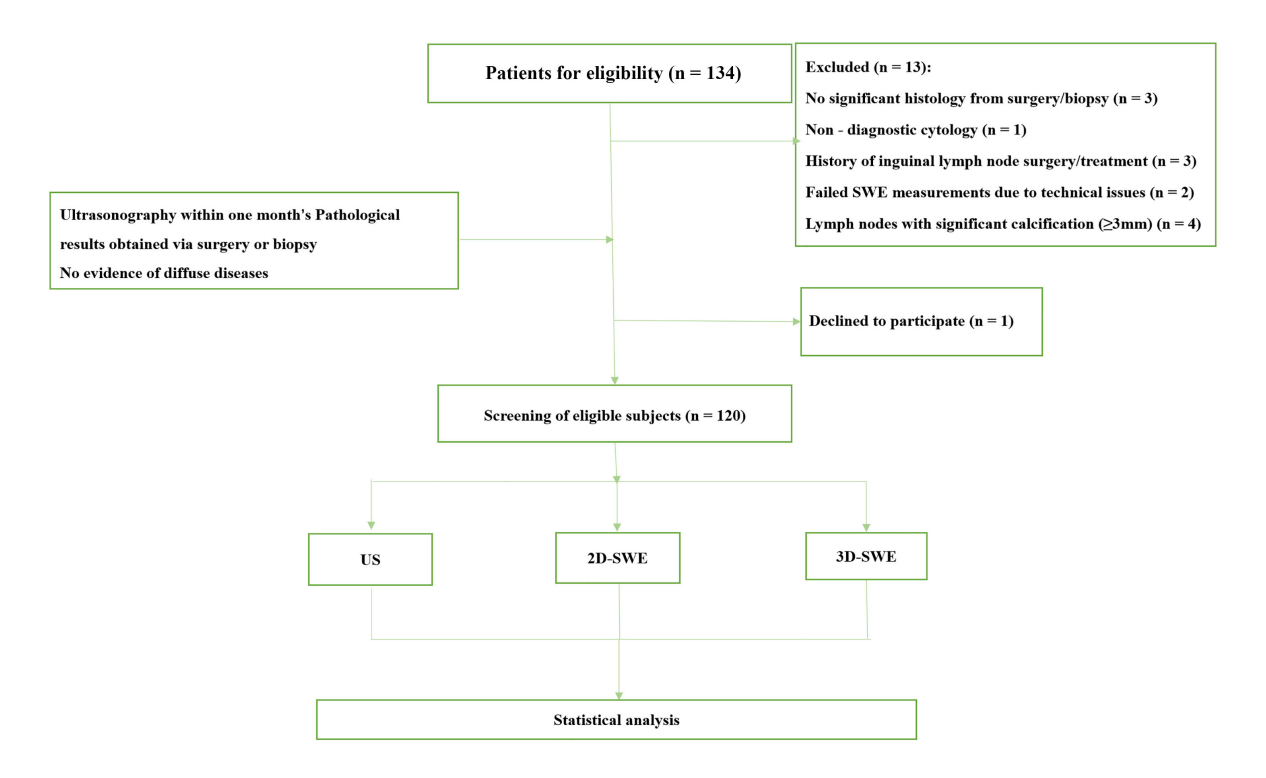


**Fig. 1. Patient flow diagram.** SWE, shear wave elastography; US, ultrasound; 2D-SWE, two-dimensional shear wave elastography; 3D-SWE, three-dimensional shear wave elastography.

22], demonstrating its potential to reduce unnecessary biopsies in suspected malignancies [23-25] and predict prognosis in certain cancer types [26-29]. Numerous clinical studies have highlighted the efficacy of two-dimensional (2D) elastography in differentiating between benign and malignant tumors [30-35], including the distinction between benign and metastatic lymph nodes [36-38]. However, conventional 2D elastography is confined to a single imaging plane, which is inadequate for assessing the complex three-dimensional spatial heterogeneity in tissue stiffness that is characteristic of metastatic lymph nodes. Three-dimensional shear wave elastography (3D-SWE) addresses this limitation by acquiring consecutive 2D images for three-dimensional (3D) reconstruction, thereby facilitating a comprehensive, volumetric quantification of elastic distribution within tissues, potentially improving diagnostic accuracy and characterization of lymph nodes [39–43]. Nonetheless, the application of 3D-SWE to evaluate ILN has yet to be explored. This study investigates the use of 3D-SWE for the assessment of ILN in gynecological cancers, positing that this approach may enhance diagnostic accuracy. The findings could establish 3D-SWE as a reliable method for assessing metastasis in ILN, thereby informing patient management.

#### 2. Materials and Methods

#### 2.1 Participants

This retrospective study was conducted from January to August in 2017, enrolling 134 patients with gynecolog-

ical cancer. The study adhered to the ethical standards outlined in the Helsinki Declaration and received approval from the institutional review board. Informed consent was obtained from all patients prior to their inclusion in the study.

The inclusion criteria were as follows: (a) ILN histopathological confirmed as benign or metastatic disease through surgical excision or ultrasound-guided core needle biopsy; (b) completion of pathological examination and diagnosis within two weeks following lymph node ultrasound; and (c) absence of diffuse systemic diseases such as lymphoma, leukemia, or other hematological malignancies.

The exclusion criteria included: (a) lymph nodes lacking adequate histological results from surgical excision or core needle biopsy within the specified timeframe; (b) patients lost to follow-up or with cytology findings classified as 'indeterminate' or 'uncertain' without subsequent histological examination; (c) prior history of ILN surgery, treatment, or invasive diagnostic procedures; (d) failure to obtain informed consent; (e) inability to perform shear wave elastography (SWE) measurements due to breath-holding difficulties or vascular pulsation artifacts; and (f) significant or coarse calcification (diameter ≥3 mm), affecting the accuracy of SWE quantification. Flow diagram summarizes the patient recruitment (Fig. 1).



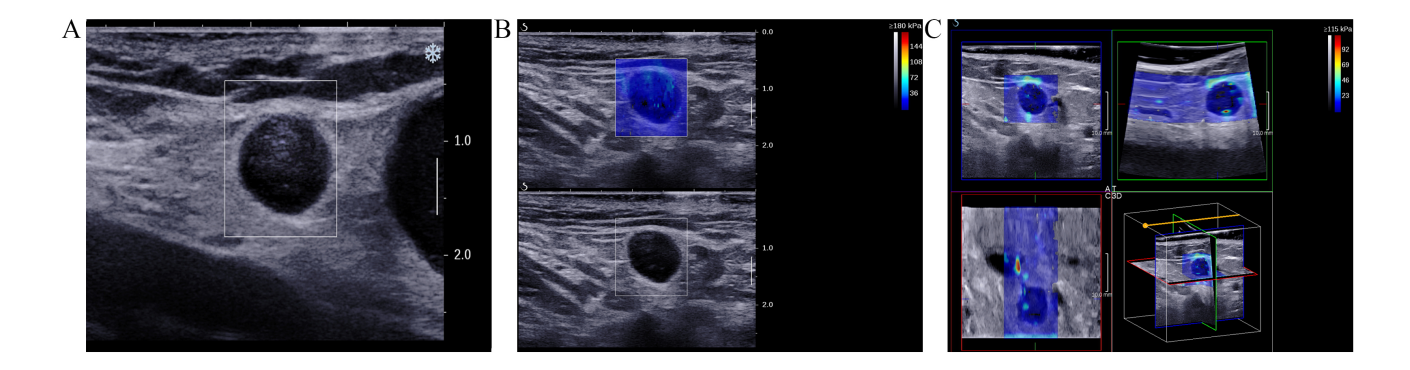


Fig. 2. Images of the inguinal lymph nodes (ILN) with metastasis originating from vulvar cancer in a 51-year-old female patient. (A) Ultrasound image illustrating indistinct corticomedullary differentiation, with a longitudinal to transverse diameter ratio exceeding 0.5. (B) 2D-SWE image. (C) Consists of orthogonal planes (transverse, coronal, and sagittal) derived from 3D-SWE images.

#### 2.2 Methods

#### 2.2.1 Conventional Ultrasound (US)

All patients were imaged using an AixPlorer ultrasound system (SuperSonic Imagine, Aix-en-Provence, France) in US, two-dimensional shear wave elastography (2D-SWE), and 3D-SWE imaging modes. Initially, a 4-15 MHz linear array transducer was used to acquire US images. Patients were positioned supine with their inguinal regions exposed for imaging, while two sonographers, Y.S. and J.D., each with over 10 years of experience, conducted comprehensive scans of the ILN. During the scanning process, the morphological characteristics of the lymph nodes—including size, internal echogenicity, cortical thickening, hilar appearance, and vascularity—were evaluated independently, with the sonographers blinded to the pathological diagnosis. Lymph node metastasis was suspected based on the presence of features including microcalcification, cystic changes, diffuse or focal hyperechogenicity, a longitudinal-to-transverse diameter ratio of less than 2, peripheral or mixed vascularity, irregular margins, or loss of the fatty hilum.

#### 2.2.2 2D-SWE

A 5–14 MHz linear probe was utilized to assess the lymph node. During the procedure, the ultrasound physician (Y.S. or J.D.) applied ultrasound gel and gently placed the transducer on the skin surface overlying the ILN. The patient was instructed to momentarily hold their breath while the sampling box was adjusted to encompass the entire structure. After stabilizing the image for 3 to 5 seconds, SWE was performed. For quantitative analysis, a 2 mm region of interest (ROI) was designated at the stiffest part of the lymph node, while avoiding calcified and liquefied regions. The Q-Box system (SuperSonic Imagine, Aix-en-Provence, France) subsequently calculated the maximum (Emax) and average (Emean) elasticity values in kilopascals (kPa) by averaging three measurements.

#### 2.2.3 3D-SWE

During the 3D-SWE examination, a 5–16 MHz volume transducer was utilized by two experienced ultrasound physicians (Y.S. and J.D.). The procedure commenced with appropriate patient preparation including positioning the patient in a supine position with the neck slightly extended. An adequate amount of ultrasound gel was applied to facilitate optimal acoustic coupling. The examination procedure mirrored that of 2D-SWE. The transducer was gently positioned over the targeted lymph node, and the sampling frame was meticulously adjusted to encompass the entire lymph node within the view. Once the appropriate settings were confirmed, including optimal depth and gain adjustments for clear visualization, the 3D-SWE mode was activated. At this stage, the transducer was held steady, and the patient was instructed to hold their breath for 3-5 seconds while the 3D image was captured to minimize motion artifacts. For quantitative analysis, the captured 3D volume was reviewed layer by layer using a tri-plane orthogonal schematic (transverse, sagittal, and coronal planes), enabling a comprehensive examination of various crosssections of the lymph node. High-quality images that accurately represented the lesion were selected for further analysis. A 2 mm ROI was subsequently designated in the most rigid part of the node, ensuring that the measurements reflected the most relevant tissue characteristics. Data collection was conducted using the Q-Box system, which facilitated the measurement of Emax and Emean values in kilopascals (kPa). Three measurements were taken from the designated ROI to derive an average value for each parameter, thereby ensuring consistency and reliability in the results. This approach aimed to enhance the accuracy of the 3D-SWE assessments and support subsequent analysis of metastatic involvement in the lymph nodes (Fig. 2).



Table 1. Elasticity Values of 2D-SWE and 3D-SWE Planes for metastatic and benign ILN.

	Metastatic $(n = 65)$	Benign $(n = 55)$	p value
2D-SWE			
Emax (kPa)	38.8 (23.6, 82.8)	17.3 (13.5, 26.5)	p < 0.0001
Emean (kPa)	31.3 (16.1, 65.4)	15.3 (11.3, 23.6)	p < 0.0001
3D transverse SWE			
Emax (kPa)	55.4 (26.0, 99.5)	23.1 (18.6, 28.4)	p < 0.0001
Emean (kPa)	34.5 (20.9, 76.8)	18.2 (15.1, 22.8)	p < 0.0001
3D sagittal SWE			
Emax (kPa)	49.8 (26.0, 91.2)	21.0 (18.1, 25.1)	p < 0.0001
Emean (kPa)	37.3 (19.6, 72.4)	18.3 (15.8, 22.7)	p < 0.0001
3D coronal SWE			
Emax (kPa)	58.2 (26.0, 86.5)	21.3 (17.5, 25.0)	p < 0.0001
Emean (kPa)	38.3 (19.4, 71.7)	18.1 (14.4, 20.4)	p < 0.0001

Emax, the maximum elasticity values; Emean, the average elasticity values.

#### 2.2.4 Statistical Analysis

Statistical analysis was conducted using SPSS version 26.0 (IBM, Chicago, IL, USA). Both Emax and Emean did not conform to a normal distribution and were therefore represented as the median (P25, P75) values. Differences in nonparametric variables were analyzed using the Wilcoxon rank-sum test, with statistical significance set at p < 0.05. Additionally, MedCalc version 20 software (MedCalc, Ostend, Belgium) was utilized to generate receiver operating characteristic (ROC) curves and to compute the area under the curve (AUC) to evaluate the diagnostic performance of the ultrasound parameters. The optimal cut-off value was identified based on the maximum Youden index, which was the point on the ROC curve that maximizes the sum of sensitivity and specificity. Interobserver agreement was evaluated using the intraclass correlation coefficient (ICC).

#### 3. Results

#### 3.1 Participant Demographics and Characterization

This study enrolled a total of 120 patients. A total of 13 participants were excluded for the following reasons: 3 had no significant histology from surgery or biopsy, 1 had non-diagnostic cytology, 3 had a history of ILN surgery or treatment, 2 had failed SWE measurements due to technical issues, and 4 had lymph nodes with significant calcification (>3 mm). Additionally, 1 participant declined to participate. The mean age of the participants was  $52.85 \pm 10.11$ years, with an age range of 35 to 71 years. The participants had 120 lymph nodes, with a mean maximum diameter of  $17.43 \pm 4.06$  mm. Among these lymph nodes, 65 were identified as metastatic, comprising 37 from cervical cancer, 9 from vulvar cancer, 11 from vaginal cancer, 5 from ovarian cancer, 1 from endometrial cancer, 1 from ovarian fibrosarcoma, and 1 from fallopian tube cancer. The remaining 55 lymph nodes were classified as benign, with 41 from cervical cancer, 9 from vulvar cancer, 2 from vaginal cancer, 2 from ovarian cancer, and 1 from endometrial cancer. Based on the reproducibility analysis, the interobserver reliability demonstrated a high level of consistency, with an ICC greater than 0.75.

#### 3.2 US Findings

A total of 56 lymph nodes were diagnosed as benign using US. Among these, 41 lymph nodes (73.21%) were pathologically confirmed as benign. Additionally, 64 lymph nodes were diagnosed as metastatic, with 50 (78.13%) confirmed pathologically as malignant. For metastatic ILN, grayscale ultrasound exhibited sensitivity of 76.92%, specificity of 74.55%, accuracy of 75.83%, positive predictive value of 78.13%, and negative predictive value of 73.21%.

#### 3.3 Elastography Parameters of 2D-SWE

The median Emax and Emean of 65 malignant lymph nodes on 2D-SWE were 38.8 (23.6, 82.8) kPa and 31.3 (16.1, 65.4) kPa, respectively. The median Emax and Emean of 55 benign lymph nodes on 2D-SWE were 17.3 (13.5, 26.5) kPa and 15.3 (11.3, 23.6) kPa, respectively. The 2D-SWE Emax and Emean for malignant lymph nodes were both higher than those for benign lymph nodes, with statistically significant differences (p < 0.0001 for both comparisons) (Table 1).

#### 3.4 Elastography Parameters of 3D-SWE

The median Emax and Emean values on the transverse plane of 3D-SWE for malignant lymph nodes were 55.4 (26.0, 99.5) kPa and 34.5 (20.9, 76.8) kPa, respectively. In contrast, the median Emax and Emean values for benign lymph nodes were 23.1 (18.6, 28.4) kPa and 18.2 (15.1, 22.8) kPa, respectively. Both Emax and Emean values were significantly higher in malignant lymph nodes than in benign lymph nodes (p < 0.0001 for both comparisons). In the sagittal plane of 3D-SWE, the median Emax and Emean for malignant lymph nodes were 49.8 (26.0, 91.2) kPa and 37.3 (19.6, 72.4) kPa, respectively. In contrast, for benign lymph



Table 2. Comparison of the diagnostic performance of the five models.

	Cut-off*	AUC	Sensitivity (%)	Specificity (%)	PPV	NPV	Accuracy	Youden's J statistic	p value
US	-	-	76.92	74.55	78.13	73.21			-
2D-SWE									
Emax	22.5	0.798 (0.715-0.866)	78.46	70.91	76.12	73.59	75.00	0.4937	p < 0.0001
Emean	16.3	0.738 (0.650-0.814)	73.85	65.45	71.64	67.93	70.00	0.3930	p < 0.0001
3D-SWE-A									
Emax	25.0	0.828 (0.748-0.891)	75.38	76.36	79.03	72.41	75.83	0.5175	p < 0.0001
Emean	19.8	0.786 (0.702-0.856)	72.31	72.73	75.81	69.00	72.50	0.4503	p < 0.0001
3D-SWE-S									
Emax	25.1	0.839 (0.760-0.899)	78.46	76.36	79.69	75.00	77.50	0.5483	p < 0.0001
Emean	19.6	0.746 (0.658-0.821)	75.38	67.27	73.13	69.81	71.67	0.4266	p < 0.0001
3D-SWE-C									
Emax	27.3	0.816 (0.734-0.880)	72.31	74.55	77.05	69.49	73.33	0.5175	p < 0.0001
Emean	21.8	0.766 (0.680-0.838)	73.85	72.73	76.19	70.18	73.33	0.4657	p < 0.0001

AUC, area under the curve; PPV, positive predictive value; NPV, negative predictive value; Emax, maximum elasticity values; Emean, average elasticity values; 3D-SWE-A, the transverse plane of 3D-SWE; 3D-SWE-S, the sagittal plane of 3D-SWE; 3D-SWE-C, the coronal plane of 3D-SWE; \*The optimal cut-off, yielding maximum sensitivity and specificity on SWE.

nodes, the median Emax and Emean values were 21.0 (18.1, 25.1) kPa and 18.3 (15.8, 22.7) kPa. Notably, both Emax and Emean were significantly higher in malignant lymph nodes compared to benign lymph nodes (p < 0.0001 for both comparisons).

In the coronal plane of 3D-SWE, the median Emax and Emean for malignant lymph nodes were 58.2 (26.0, 86.5) kPa and 38.3 (19.4, 71.7) kPa, respectively. In contrast, for benign lymph nodes, the median Emax and Emean were 21.3 (17.5, 25.0) kPa and 18.1 (14.4, 20.4) kPa, respectively. Notably, both Emax and Emean values on the coronal plane were significantly higher for malignant lymph nodes than for benign lymph nodes (p < 0.0001 for both comparisons) (Table 1).

## 3.5 Diagnostic Performance of the Quantitative 2D-SWE and 3D-SWE Findings

The ROC curves were generated using pathology results as the reference standard. The AUC of the Emax value of 2D-SWE for differentiating between benign and metastatic lymph nodes was 0.798 (95% confidence interval [CI]: 0.715–0.866). The AUCs for the Emax values of the transverse, sagittal, and coronal planes of 3D-SWE were 0.828 (95% CI: 0.748–0.891), 0.839 (95% CI: 0.760–0.899), and 0.816 (95% CI: 0.734–0.880), respectively (Fig. 3). No significant differences were observed between these AUCs (p > 0.05 for all comparisons).

The AUC for Emean in 2D-SWE was 0.738 (95% CI: 0.650–0.814). The AUCs for Emean in the transverse, sagittal, and coronal planes of 3D-SWE were 0.786 (95% CI: 0.702–0.856), 0.746 (95% CI: 0.658–0.821), and 0.766 (95% CI: 0.680–0.838), respectively. There were no significant differences observed between 2D-SWE and the three planes of 3D-SWE (p > 0.05 for all comparisons). In both 2D-SWE and 3D-SWE, the AUC for Emax was higher

than that for Emean in differentiating between benign and metastatic lymph nodes. For 2D-SWE, the AUCs for Emax and Emean were 0.798 (95% CI: 0.715–0.866) and 0.738 (95% CI: 0.650–0.814), respectively. In 3D-SWE, the AUCs for Emax and Emean were as follows: for the transverse plane, Emax was 0.828 (95% CI: 0.748–0.891) and Emean was 0.786 (95% CI: 0.702–0.856); for the sagittal plane, Emax was 0.839 (95% CI: 0.760–0.899) and Emean was 0.746 (95% CI: 0.658–0.821); and for the coronal plane, Emax was 0.816 (95% CI: 0.734–0.880) and Emean was 0.766 (95% CI: 0.680–0.838).

When differentiating between benign and malignant lymph nodes, the Emax index in the sagittal plane of 3D-SWE demonstrates higher sensitivity and specificity compared to US. The optimal cut-off values for both 2D-SWE and 3D-SWE parameters, as well as their corresponding diagnostic performance, are summarized in Table 2.

#### 4. Discussion

3D-SWE utilizes ultrasound-generated shear waves to quantify tissue elasticity. By overcoming the limitations of 2D-SWE, such as its reliance on a single imaging plane and lack of anatomical context, 3D-SWE provides a more comprehensive model of tissue elasticity through multiplanar reconstruction. This technique facilitates intuitive visualization of lesions in transverse, coronal, and sagittal planes, thereby allowing for a more detailed description of tissue hardness [44]. By providing insights into tissue stiffness and elasticity, 3D-SWE enhances the diagnosis of small structures and deep organs.

In this study, we evaluated the efficacy of 3D-SWE for detecting ILN metastases in gynecological malignancies, which has not been extensively explored in the literature. The 3D-SWE technology demonstrated higher sensitivity and specificity compared to US, indicating its su-



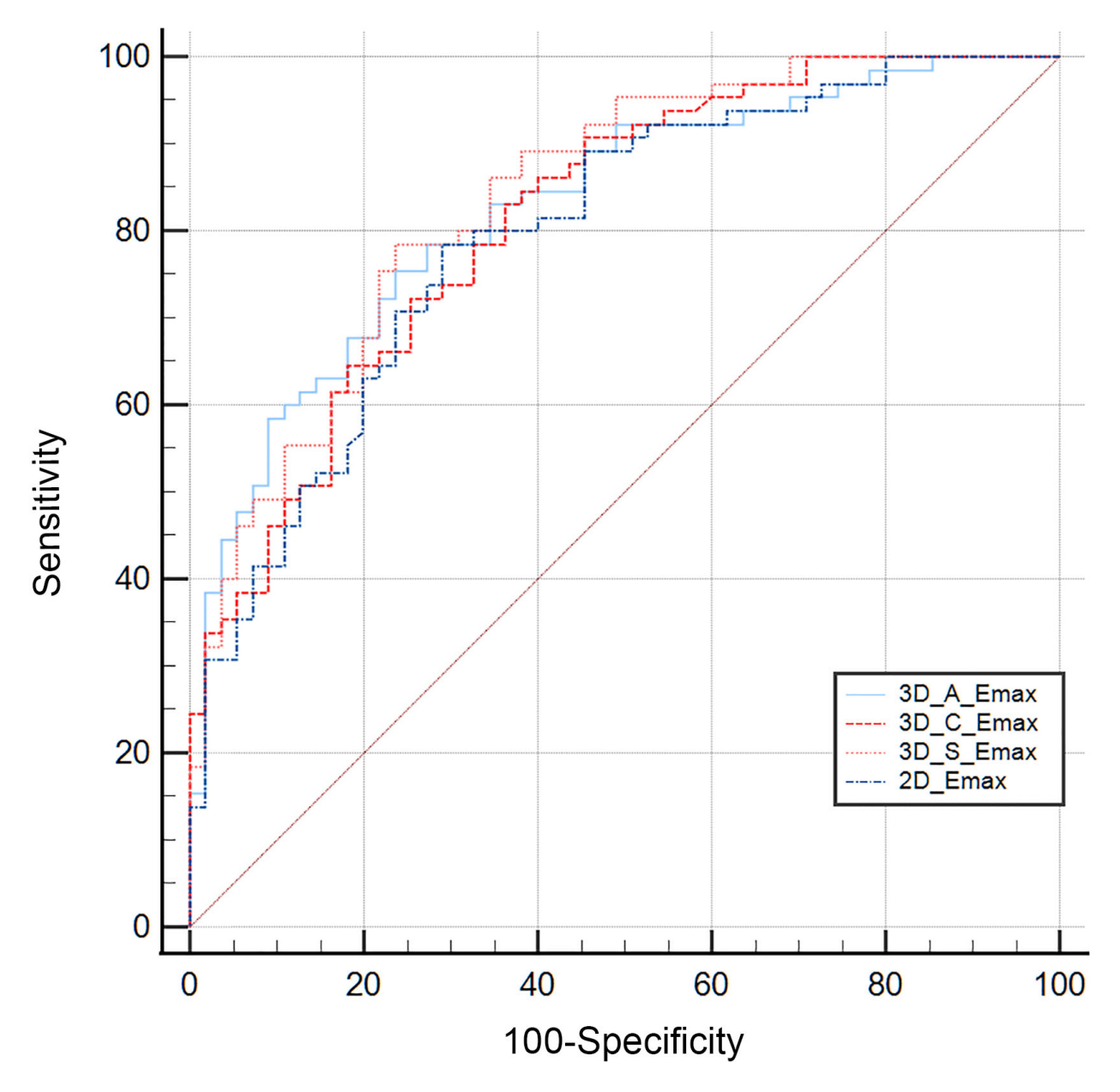


Fig. 3. The ROC curve for the quantitative parameters of 2D-SWE and 3D-SWE in the diagnosis of metastatic ILN. ROC, receiver operating characteristic; ILN, inguinal lymph nodes; 3D\_A\_Emax, the maximum elasticity modulus in the transverse plane of 3D-SWE; 3D\_C\_Emax, the maximum elasticity modulus in the coronal plane of 3D-SWE; 3D\_S\_Emax, the maximum elasticity modulus in the sagittal plane of 3D-SWE; 2D\_Emax, the maximum elasticity modulus of 2D-SWE.

perior performance in differentiating between benign and metastatic lymph nodes. This enhanced performance may be attributed to 3D-SWE's ability to quantitatively assess tissue elasticity, reflecting pathophysiological changes such as increased cell density and extracellular matrix proliferation, which are characteristic of malignant tumors. Furthermore, the excellent interobserver agreement (with an ICC of greater than 0.75) further substantiates the reliability and robustness of 3D-SWE for quantitative elastography.

In this study, we demonstrated the capability of 2D-SWE to quantitatively differentiate between benign and metastatic ILN based on stiffness measurements. The

significantly elevated Emax and Emean values observed in metastatic lymph nodes are consistent with findings from previous studies [45–47]. Kawahara *et al.* [48] detected high shear wave velocities in ILN during the micrometastatic phase, reflecting tissue stiffening associated with extracellular matrix remodeling induced by tumor growth. The ability of 2D-SWE to identify tissue stiffening, even when the nodal capsule remains intact, highlights its diagnostic potential for early detection of metastatic progression, before structural changes are evident [48]. However, Suh *et al.* [49] noted that the prevalence of malignant lymph nodes significantly influences the heterogene-



ity observed in 2D-SWE studies, suggesting the necessity for standardized protocols, particularly in terms of measurement techniques and thresholds for malignancy.

When interpreting elastography measurements, it is essential to consider various factors that may influence the accuracy and consistency of the results. In this study, both benign and malignant ILN exhibited higher Emax and Emean values when assessed using 3D-SWE compared to 2D-SWE. This finding aligns with other investigations indicating that lesion stiffness values measured via 3D-SWE are generally greater than those obtained with 2D-SWE [50]. Further analysis suggests that the heavier transducer mass and the requirement for additional coupling agents in 3D-SWE may exert extra external pressure on the tissue, contributing to higher measured stiffness values. Additionally, several factors that influence the quality of 3D-SWE images include the amount of application of pressure, lesion location, pathological characteristics, maximal diameter, longest perpendicular depth from the skin, and the thickness of the prefocal tissue [51]. These factors also affect 2D-SWE measurements, although to a lesser extent. Furthermore, the cut-off stiffness values obtained for ILN in our study were lower than those commonly reported for cervical lymph nodes. This discrepancy is likely due to anatomical differences between the groin and neck regions, such as the irregularity of the skin, the presence of large vessels and the trachea, as well as the rigidity of pulsating vascular walls and tracheal cartilage, all of which typically yield higher stiffness measurements in the neck. In contrast, the flatter skin and looser subcutaneous tissues of the groin result in lower stiffness readings compared to the neck region. Studies on SWE of canine lymph nodes by Favril et al. [52] support this observation, demonstrating higher inter- and intra-observer consistency for ILNs compared to mandibular and popliteal lymph nodes, further highlighting the influence of anatomical factors on elastography measurements.

Malignant lesions often exhibit significant heterogeneity in tissue architecture, which can complicate the assessment of tumor stiffness and detection of regions with higher malignancy potential. However, 3D-SWE provides a multidimensional representation of stiffness variations within the mass, enhancing the detection of nonuniform stiffness variations, which is crucial for identifying malignant areas that may otherwise be missed using conventional methods. Studies conducted by Tian et al. [53] and Zhao et al. [54] demonstrated that 3D-SWE is superior to 2D-SWE in evaluating lesion homogeneity and specificity, and also outperformed US in diagnostic performance, particularly in detecting irregularities within heterogeneous tumors. Nevertheless, research findings have been inconsistent regarding the clinical advantages of either 2D-SWE or 3D-SWE, particularly with respect to their ability to quantify breast tumors and their overall diagnostic accuracy [55– 57]. Yin et al. [58] reported that Young's modulus value of 3D-SWE did not significantly differ across the transverse, sagittal, and coronal planes in muscle tissue. However, 3D-SWE's ability of depicting tissue from multiple angles allowed for more accurate characterization of its spatial properties. Chen *et al.* [44,59] found that the coronal plane exhibited the most pronounced elastic property variations and was least affected by pressure artifacts, thus providing optimal accuracy. In contrast, Wang *et al.* [57] reported that the sagittal plane demonstrated superior diagnostic capability compared to the transverse and coronal planes [39,60].

Our study also observed no significant differences in quantitative parameters across the three planes (p > 0.05), although the sagittal plane yielded the highest Emax AUC value. Differences in the imaging plane and imaging direction may contribute to the observed variability. Furthermore, the structural heterogeneity of tumors, including anisotropy in malignant neoplasms, as well as variations among tumor subtypes, affect stiffness and further complicate the interpretation of elastography results. Current evidence increasingly supports Emax as the preferred index for assessing breast lesions. Gao et al. [61] systematically reviewed four databases following the preferred reporting items for systematic review and meta-analysis (PRISMA) guidelines to evaluate the efficacy of SWE parameters in identifying malignant lymph nodes, finding that Emax and standard deviation of elasticity values (Esd) exhibited the highest sensitivity, while Emean provided optimal specificity. Song et al. [29] identified significant associations between higher Emax values and lymphovascular invasion, as well as larger pathological areas, suggesting that SWE could be a valuable tool for enhancing prognosis prediction in breast cancer. Analyses by Li et al. [62] indicated that larger tumors were often associated with elevated Emax and Emean values, with Emax levels in the lymphovascular invasion group exceeding those in the negative group. Furthermore, investigations by Xue et al. [63] demonstrated that Emax outperformed Emean in sensitivity, specificity, and accuracy in diagnosing breast lesions, consistent with our study findings. This superiority may be attributed to the most rigid part of the tumor consistently being located within the region of interest, leading to relatively stable Emax values, while other parameters, such as Emean, are more susceptible to fluctuations due to segmentation variability [64]. Some studies have shown that considering the characteristics of the peripheral region of lymph nodes can improve the diagnostic accuracy for metastatic lymph nodes [65]. This could be a valuable direction for further exploration in future studies.

#### Limitations

Due to the retrospective design of this study, the examined population may not fully represent the broader population of patients with gynecological malignancies. Additionally, ultrasound imaging is influenced by both the operator's technique and the machine settings. Future research



should involve multicenter randomized trials with larger, more diverse sample sizes to better validate and generalize these findings.

#### 5. Conclusions

3D-SWE effectively differentiates between benign and metastatic lymph nodes by quantitatively assessing the stiffness of ILNs in patients with gynecological tumors. As a reliable diagnostic tool for lymph nodes, 3D-SWE can reduce the need for invasive biopsy procedures while providing valuable non-invasive information.

#### **Abbreviations**

2D SWE, two-dimensional shear wave elastography; 3D SWE, three-dimensional shear wave elastography; ILN, inguinal lymph node; US, conventional ultrasound; CT, computed tomography.

### Availability of Data and Materials

The data that support the findings of this study are available on request from the corresponding author.

#### **Author Contributions**

YPS and JLD performed the investigation, resourced the data, curated the data, wrote the original draft of the manuscript, and created the visualizations. JLD conducted a formal analysis and reviewed and edited the writing. JML carried out the methodology and validation work. ML conceptualized the study, supervised the research, and administered the project. All authors read and agreed to the published version of the manuscript. All authors contributed to editorial changes in the manuscript. All authors have participated sufficiently in the work and agreed to be accountable for all aspects of the work.

#### **Ethics Approval and Consent to Participate**

The study was conducted by the declaration of Helsinki and approved by the medical ethics committee of Sichuan Cancer Hospital (Protocol code SCCHEC-03-2022-007 and approval date 2022-03-01). Informed consent was obtained from the participants included in the study.

#### Acknowledgment

This project's success owes much to my team. We overcame difficulties together. Special thanks to our leader for leading the way and making everything organized.

#### **Funding**

This research was funded by the Youth Fund of Sichuan Medical Association, grant number Q17075.

#### **Conflict of Interest**

The authors declare no conflict of interest.

#### References

- Suneja G, Viswanathan A. Gynecologic malignancies. Hematology/oncology Clinics of North America. 2020; 34: 71–89. https://doi.org/10.1016/j.hoc.2019.08.018.
- [2] Buskwofie A, David-West G, Clare CA. A review of cervical cancer: incidence and disparities. Journal of the National Medical Association. 2020; 112: 229–232. https://doi.org/10.1016/j. inma.2020.03.002.
- [3] Bhatla N, Aoki D, Sharma DN, Sankaranarayanan R. Cancer of the cervix uteri: 2021 update. International Journal of Gynaecology and Obstetrics: The Official Organ of the International Federation of Gynaecology and Obstetrics. 2021; 155 Suppl 1: 28–44. https://doi.org/10.1002/ijgo.13865.
- [4] Brooks RA, Fleming GF, Lastra RR, Lee NK, Moroney JW, Son CH, et al. Current recommendations and recent progress in endometrial cancer. CA: A Cancer Journal for Clinicians. 2019; 69: 258–279. https://doi.org/10.3322/caac.21561.
- [5] Raglan O, Kalliala I, Markozannes G, Cividini S, Gunter MJ, Nautiyal J, et al. Risk factors for endometrial cancer: An umbrella review of the literature. International Journal of Cancer. 2019; 145: 1719–1730. https://doi.org/10.1002/ijc.31961.
- [6] Crosbie EJ, Kitson SJ, McAlpine JN, Mukhopadhyay A, Powell ME, Singh N. Endometrial cancer. Lancet (London, England). 2022; 399: 1412–1428. https://doi.org/10.1016/ S0140-6736(22)00323-3.
- [7] Siegel RL, Miller KD, Fuchs HE, Jemal A. Cancer statistics, 2022. CA: A Cancer Journal for Clinicians. 2022; 72: 7–33. https://doi.org/10.3322/caac.21708.
- [8] Colombo N, Sessa C, du Bois A, Ledermann J, McCluggage WG, McNeish I, et al. ESMO-ESGO consensus conference recommendations on ovarian cancer: pathology and molecular biology, early and advanced stages, borderline tumours and recurrent disease. Annals of Oncology: Official Journal of the European Society for Medical Oncology. 2019; 30: 672–705. https://doi.org/10.1093/annonc/mdz062.
- [9] Mix JM, Gopalani SV, Simko S, Saraiya M. Trends in HPVand non-HPV-associated vulvar cancer incidence, United States, 2001-2017. Preventive Medicine. 2022; 164: 107302. https://doi.org/10.1016/j.ypmed.2022.107302.
- [10] Kehoe S, Bhatla N. FIGO Cancer Report 2021. International Journal of Gynaecology and Obstetrics: The Official Organ of the International Federation of Gynaecology and Obstetrics. 2021; 155 Suppl 1: 5–6. https://doi.org/10.1002/ijgo.13882.
- [11] Wang YZ, Yao YY, Liang ZQ Anatomy and physiological function of female pelvic, abdominal aorta and inguinal lymph nodes. Chinese Journal of Practical Gynecology and Obstetrics. 2017; 33: 1241–1245. https://doi.org/10.19538/j.fk2017120108.
- [12] Pelligra S, Scaletta G, Cianci S, Gueli Alletti S, Restaino S, Fagotti A, et al. Update on new imaging technologies in sentinel node detection. Minerva Ginecologica. 2020; 72: 404–412. https://doi.org/10.23736/S0026-4784.20.04707-3.
- [13] Spijkers S, Staats JM, Littooij AS, Nievelstein RAJ. Abdominal lymph node size in children at computed tomography. Pediatric Radiology. 2020; 50: 1263–1270. https://doi.org/10.1007/s00247-020-04715-z.
- [14] Garganese G, Fragomeni SM, Pasciuto T, Leombroni M, Moro F, Evangelista MT, et al. Ultrasound morphometric and cytologic preoperative assessment of inguinal lymph-node status in women with vulvar cancer: MorphoNode study. Ultrasound in Obstetrics & Gynecology: The Official Journal of the International Society of Ultrasound in Obstetrics and Gynecology. 2020; 55: 401–410. https://doi.org/10.1002/uog.20378.
- [15] Verri D, Moro F, Fragomeni SM, Zaçe D, Bove S, Pozzati F, et al.

  The role of ultrasound in the evaluation of inguinal lymph nodes in patients with vulvar cancer: A systematic review and meta-



- analysis. Cancers. 2022; 14: 3082. https://doi.org/10.3390/cancers14133082.
- [16] Sakamoto T, Ito S, Uchida K, Kuroda H, Minoji T, Endo A, et al. P1500Evaluation of hepatic congestion on liver stiffness in patients with heart failure by shear wave and strain imaging (combinational elastography). European Heart Journal. 2018; 39: ehy565.P1500. https://doi.org/10.1093/eurheartj/ehy565.P1500.
- [17] Park SY, Choi JS, Han BK, Ko EY, Ko ES. Shear wave elastography in the diagnosis of breast non-mass lesions: factors associated with false negative and false positive results. European Radiology. 2017; 27: 3788–3798. https://doi.org/10.1007/s00330-017-4763-6.
- [18] Swan KZ, Nielsen VE, Bonnema SJ. Evaluation of thyroid nodules by shear wave elastography: A review of current knowledge. Journal of Endocrinological Investigation. 2021; 44: 2043–2056. https://doi.org/10.1007/s40618-021-01570-z.
- [19] Chen ZT, Jin FS, Guo LH, Li XL, Wang Q, Zhao H, et al. Value of conventional ultrasound and shear wave elastography in the assessment of muscle mass and function in elderly people with type 2 diabetes. European Radiology. 2023; 33: 4007–4015. ht tps://doi.org/10.1007/s00330-022-09382-2.
- [20] Anbarasan T, Wei C, Bamber JC, Barr RG, Nabi G. Characterisation of prostate lesions using transrectal shear wave elastography (SWE) ultrasound imaging: A systematic review. Cancers. 2021; 13: 122. https://doi.org/10.3390/cancers13010122.
- [21] Dikici AS, Ustabasioglu FE, Delil S, Nalbantoglu M, Korkmaz B, Bakan S, *et al.* Evaluation of the tibial nerve with shear-wave elastography: A potential sonographic method for the diagnosis of diabetic peripheral neuropathy. Radiology. 2017; 282: 494–501. https://doi.org/10.1148/radiol.2016160135.
- [22] Feng Q, Chaemsaithong P, Duan H, Ju X, Appiah K, Shen L, et al. Screening for spontaneous preterm birth by cervical length and shear-wave elastography in the first trimester of pregnancy. American Journal of Obstetrics and Gynecology. 2022; 227: 500.e1–500.e14. https://doi.org/10.1016/j.ajog.2022.04.014.
- [23] Golatta M, Pfob A, Büsch C, Bruckner T, Alwafai Z, Balleyguier C, *et al.* The potential of combined shear wave and strain elastography to reduce unnecessary biopsies in breast cancer diagnostics An international, multicentre trial. European Journal of Cancer (Oxford, England: 1990). 2022; 161: 1–9. https://doi.org/10.1016/j.ejca.2021.11.005.
- [24] Pfob A, Sidey-Gibbons C, Barr RG, Duda V, Alwafai Z, Balleyguier C, et al. Intelligent multi-modal shear wave elastography to reduce unnecessary biopsies in breast cancer diagnosis (INSPiRED 002): A retrospective, international, multicentre analysis. European Journal of Cancer (Oxford, England: 1990). 2022; 177: 1–14. https://doi.org/10.1016/j.ejca.2022.09.018.
- [25] Tanaka T, Kamata M, Fukaya S, Hayashi K, Fukuyasu A, Ishikawa T, et al. Usefulness of real-time elastography for diagnosing lymph node metastasis of skin cancer: does elastography potentially eliminate the need for sentinel lymph node biopsy in squamous cell carcinoma? Journal of the European Academy of Dermatology and Venereology: JEADV. 2020; 34: 754–761. https://doi.org/10.1111/jdv.15955.
- [26] Ventura C, Baldassarre S, Cerimele F, Pepi L, Marconi E, Ercolani P, et al. 2D shear wave elastography in evaluation of prognostic factors in breast cancer. La Radiologia Medica. 2022; 127: 1221–1227. https://doi.org/10.1007/s11547-022-01559-5.
- [27] Bae SJ, Cha YJ, Eun NL, Ji J, Jeong J. The value of shear-wave elastography for prediction of tumor-infiltrating lymphocytes in patients with breast cancer. European Journal of Cancer. 2020; 138: S103. https://doi.org/10.1016/S0959-8049(20)30811-X.
- [28] Gu J, Polley EC, Denis M, Carter JM, Pruthi S, Gregory AV, *et al*. Early assessment of shear wave elastography parameters foresees the response to neoadjuvant chemotherapy in patients

- with invasive breast cancer. Breast Cancer Research: BCR. 2021; 23: 52. https://doi.org/10.1186/s13058-021-01429-4.
- [29] Song EJ, Sohn YM, Seo M. Tumor stiffness measured by quantitative and qualitative shear wave elastography of breast cancer. The British Journal of Radiology. 2018; 91: 20170830. https://doi.org/10.1259/bjr.20170830.
- [30] Zhang X, Zheng Y, Li J, Zhang B. Application of the shear wave elastography in the assessment of carotid body tumors: A preliminary study. Frontiers in Oncology. 2023; 12: 1053236. https://doi.org/10.3389/fonc.2022.1053236.
- [31] Liang JF, Feng MC, Luo PP, Guan JY, Chen GF, Wu SY, *et al.* High-frequency ultrasound and shear wave elastography in quantitative differential diagnosis of high-risk and low-risk basal cell carcinomas. Journal of Ultrasound in Medicine: Official Journal of the American Institute of Ultrasound in Medicine. 2022; 41: 1447–1454. https://doi.org/10.1002/jum.15829.
- [32] Barr RG, Engel A, Kim S, Tran P, De Silvestri A. Improved breast 2D SWE algorithm to eliminate false-negative cases. Investigative Radiology. 2023; 58: 703–709. https://doi.org/10. 1097/RLI.000000000000000972.
- [33] Dudea-Simon M, Dudea SM, Ciortea R, Malutan A, Mihu D. Elastography of the uterine cervix in gynecology: normal appearance, cervical intraepithelial neoplasia and cancer. A systematic review. Medical Ultrasonography. 2021; 23: 74–82. https://doi.org/10.11152/mu-2646.
- [34] Barr RG. Future of breast elastography. Ultrasonography (Seoul, Korea). 2019; 38: 93–105. https://doi.org/10.14366/usg.18053.
- [35] Tyloch DJ, Tyloch JF, Adamowicz J, Neska-Długosz I, Grzanka D, Van Breda S, et al. Comparison of strain and shear wave elastography in prostate cancer detection. Ultrasound in Medicine & Biology. 2023; 49: 889–900. https://doi.org/10.1016/j.ultrasmedbio.2022.11.015.
- [36] Sun Y, Wang W, Mi C, Zhang Q, Zhang K. Differential diagnosis value of shear-wave elastography for superficial enlarged lymph nodes. Frontiers in Oncology. 2022; 12: 908085. https://doi.org/ 10.3389/fonc.2022.908085.
- [37] Jiang M, Li CL, Luo XM, Chuan ZR, Chen RX, Tang SC, et al. Radiomics model based on shear-wave elastography in the assessment of axillary lymph node status in early-stage breast cancer. European Radiology. 2022; 32: 2313–2325. https://doi.org/10.1007/s00330-021-08330-w.
- [38] Li J, Nian C, Ze-Ming X, Jingwen Z, Kemin H. Developing and validating deep learning-based heterogeneous model to improve diagnostic performance of ultrasound elastography for axillary lymph node metastasis of early breast cancer. Journal of Clinical Oncology. 2021; 39: e12583. https://doi.org/10.1200/JCO. 2021.39.15 suppl.e12583.
- [39] Han RJ, Du J, Li FH, Zong HR, Wang JD, Shen YL, et al. Comparisons and combined application of two-dimensional and three-dimensional real-time shear wave elastography in diagnosis of thyroid nodules. Journal of Cancer. 2019; 10: 1975–1984. https://doi.org/10.7150/jca.30135.
- [40] Xu J, Zhang L, Wen W, He Y, Wei T, Zheng Y, et al. Evaluation of standard breast ultrasonography by adding two-dimensional and three-dimensional shear wave elastography: A prospective, multicenter trial. European Radiology. 2024; 34: 945–956. http s://doi.org/10.1007/s00330-023-10057-9.
- [41] Shoji S, Hashimoto A, Nakamura T, Hiraiwa S, Sato H, Sato Y, et al. Novel application of three-dimensional shear wave elastography in the detection of clinically significant prostate cancer. Biomedical Reports. 2018; 8: 373–377. https://doi.org/10.3892/br.2018.1059.
- [42] Marcon J, Trottmann M, Rübenthaler J, D'Anastasi M, Stief CG, Reiser MF, et al. Three-dimensional vs. two-dimensional shearwave elastography of the testes - preliminary study on a healthy collective. Clinical Hemorheology and Microcirculation. 2016;



- 64: 447-456. https://doi.org/10.3233/CH-168115.
- [43] Götschi T, Franchi MV, Schulz N, Fröhlich S, Frey WO, Snedeker JG, et al. Altered regional 3D shear wave velocity patterns in youth competitive alpine skiers suffering from patellar tendon complaints a prospective case-control study. European Journal of Sport Science. 2023; 23: 1068–1076. https://doi.org/10.1080/17461391.2022.2088404.
- [44] Chen Y, Gao Y, Wang F, Li N, Miao A, Zhi W, et al. Quantitative features and diagnostic value of 3-dimensional shear wave elastography in breast lesions. Chinese Journal of Ultrasonography. 2017; 26: 613–617. https://doi.org/10.3760/cma.j.issn.1004-4477.2017.07.013.
- [45] You J, Chen J, Xiang F, Song Y, Khamis S, Lu C, *et al.* The value of quantitative shear wave elastography in differentiating the cervical lymph nodes in patients with thyroid nodules. Journal of Medical Ultrasonics (2001). 2018; 45: 251–259. https://doi.org/10.1007/s10396-017-0819-0.
- [46] Jung WS, Kim JA, Son EJ, Youk JH, Park CS. Shear wave elastography in evaluation of cervical lymph node metastasis of papillary thyroid carcinoma: elasticity index as a prognostic implication. Annals of Surgical Oncology. 2015; 22: 111–116. https://doi.org/10.1245/s10434-014-3627-4.
- [47] Desmots F, Fakhry N, Mancini J, Reyre A, Vidal V, Jacquier A, et al. Shear wave elastography in head and neck lymph node assessment: image quality and diagnostic impact compared with B-mode and Doppler ultrasonography. Ultrasound in Medicine & Biology. 2016; 42: 387–398. https://doi.org/10.1016/j.ultrasmedbio.2015.10.019.
- [48] Kawahara Y, Togawa Y, Yamamoto Y, Wakabayashi S, Matsue H, Inafuku K. Usefulness of 2-D shear wave elastography for the diagnosis of inguinal lymph node metastasis of malignant melanoma and squamous cell carcinoma. The Journal of Dermatology. 2020; 47: 1312–1316. https://doi.org/10.1111/1346-8138.15545.
- [49] Suh CH, Choi YJ, Baek JH, Lee JH. The diagnostic performance of shear wave elastography for malignant cervical lymph nodes: A systematic review and meta-analysis. European Radiology. 2017; 27: 222–230. https://doi.org/10.1007/ s00330-016-4378-3.
- [50] Lee SH, Chang JM, Kim WH, Bae MS, Cho N, Yi A, *et al.* Differentiation of benign from malignant solid breast masses: comparison of two-dimensional and three-dimensional shearwave elastography. European Radiology. 2013; 23: 1015–1026. https://doi.org/10.1007/s00330-012-2686-9.
- [51] Tong WJ, Luo J, Li JY, FS Pan, Xie XY, Zheng YL. Impact factors of imaging quality of three-dimensional shear wave elastography in focal breast lesions. Chinese Journal of Medical Imaging Technology. 2019; 35: 1017–1021. https://doi.org/10.3760/cma.j.issn.1004-4477.2017.07.013.
- [52] Favril S, de Rooster H, Broeckx BJG, Stock E, Vanderperren K. Shear wave velocity measurements obtained in different regions are repeatable for presumed normal canine lymph nodes: A pilot study. Veterinary Radiology & Ultrasound: The Official Journal of the American College of Veterinary Radiology and the International Veterinary Radiology Association. 2022; 63: 102–110. https://doi.org/10.1111/vru.13021.
- [53] Tian J, Liu Q, Wang X, Xing P, Yang Z, Wu C. Application of 3D and 2D quantitative shear wave elastography (SWE) to differentiate between benign and malignant breast masses. Scientific Reports. 2017; 7: 41216. https://doi.org/10.1038/srep41216.
- [54] Zhao CK, Chen SG, Alizad A, He YP, Wang Q, Wang D, et

- al. Three-dimensional shear wave elastography for differentiating benign from malignant thyroid nodules. Journal of Ultrasound in Medicine: Official Journal of the American Institute of Ultrasound in Medicine. 2018; 37: 1777–1788. https://doi.org/10.1002/jum.14531.
- [55] Youk JH, Gweon HM, Son EJ, Chung J, Kim JA, Kim EK. Three-dimensional shear-wave elastography for differentiating benign and malignant breast lesions: comparison with two-dimensional shear-wave elastography. European Radiology. 2013; 23: 1519–1527. https://doi.org/10.1007/s00330-012-2736-3.
- [56] Choi HY, Sohn YM, Seo M. Comparison of 3D and 2D shear-wave elastography for differentiating benign and malignant breast masses: focus on the diagnostic performance. Clinical Radiology. 2017; 72: 878–886. https://doi.org/10.1016/j.crad.2017.04.009.
- [57] Wang Q, Li XL, He YP, Alizad A, Chen S, Zhao CK, et al. Three-dimensional shear wave elastography for differentiation of breast lesions: An initial study with quantitative analysis using three orthogonal planes. Clinical Hemorheology and Microcirculation. 2019; 71: 311–324. https://doi.org/10.3233/CH -180388.
- [58] Yin L, Lu R, Cao W, Zhang L, Li W, Sun H, et al. Three-Dimensional Shear Wave Elastography of Skeletal Muscle: Pre-liminary Study. Journal of ultrasound in medicine: official journal of the American Institute of Ultrasound in Medicine. 2018; 37: 2053–2062. https://doi.org/10.1002/jum.14559.
- [59] Chen YL, Chang C, Zeng W, Wang F, Chen JJ, Qu N. 3-Dimensional shear wave elastography of breast lesions: Added value of color patterns with emphasis on crater sign of coronal plane. Medicine. 2016; 95: e4877. https://doi.org/10.1097/MD .000000000000004877.
- [60] Hu Z, Lu M, Wang X, Yang W, Fan Y, Li T, et al. Diagnostic value of different 3-D shear wave elastography sections in the diagnosis of thyroid nodules. Ultrasound in Medicine & Biology. 2022; 48: 1957–1965. https://doi.org/10.1016/j.ultrasmedbio.2022.05.036.
- [61] Gao Y, Zhao Y, Choi S, Chaurasia A, Ding H, Haroon A, et al. Evaluating different quantitative shear wave parameters of ultrasound elastography in the diagnosis of lymph node malignancies: A systematic review and meta-analysis. Cancers. 2022; 14: 5568. https://doi.org/10.3390/cancers14225568.
- [62] Li J, Sun B, Li Y, Li S, Wang J, Zhu Y, et al. Correlation analysis between shear-wave elastography and pathological profiles in breast cancer. Breast Cancer Research and Treatment. 2023; 197: 269–276. https://doi.org/10.1007/s10549-022-06804-z.
- [63] Xue X, Li J, Wan W, Shi X, Zheng Y. Kindlin-2 could influence breast nodule elasticity and improve lymph node metastasis in invasive breast cancer. Scientific Reports. 2017; 7: 6753. https://doi.org/10.1038/s41598-017-07075-1.
- [64] Xue XW, Li JL, Wan WB, Li XK. Molecular mechanisms of breast nodule stiffness. Zhongguo yi xue ke xue yuan xue bao Acta Academiae Medicinae Sinicae. 2018; 40: 279–283. (In Chinese). http://journal13.magtechjournal.com/yxkxy/EN/ PDF/10.3881/j.issn.1000-503X.2018.02.020.
- [65] Mohammadi A, Mirza-Aghazadeh-Attari M, Faeghi F, Homayoun H, Abolghasemi J, Vogl TJ, et al. Tumor microenvironment, radiology, and artificial intelligence: should we consider tumor periphery? Journal of Ultrasound in Medicine: Official Journal of the American Institute of Ultrasound in Medicine. 2022; 41: 3079–3090. https://doi.org/10.1002/jum.16086.

